

## WIDELY-TUNABLE LASER-SIDEBAND THz SOURCE FOR SPECTROSCOPY & LO APPLICATIONS

Eric R. Mueller

DeMaria ElectroOptics Systems, Inc.  
1280 Blue Hills Ave.  
Bloomfield, CT 06002  
(806) 243-9557

Jeffrey L. Hesler, Thomas W. Crowe,  
David S. Kurtz & Robert M. Weikle, II  
Applied Electrophysics Laboratories  
Department of Electrical Engineering  
University of Virginia  
Charlottesville, VA 22901

### Abstract

There has been a recent resurgence of interest in spectroscopy in the THz. The development of "short-pulse" THz sources, and the measurements made with these sources, have pointed to a number of possible applications for THz imaging and spectroscopy in biology, medicine, and semiconductor device packaging characterization. While the "short-pulse" sources offer wide-range, low resolution, THz coverage, they have a number of drawbacks for measurement applications. The work described here represents an alternative that avoids many of these drawbacks.

The work outlined in this paper marries the recent developments in high-reliability, compact THz lasers,<sup>1, 2</sup> with recent advances in Schottky-based sideband generators,<sup>3, 4</sup> to yield a reliable, potentially milliwatt-level, tunable THz source. While this work has been focussed on spectroscopy applications, the results can also be applied to provide tunable THz local oscillators.

Preliminary results & modeling for the tuning range and fixed-wavelength operating range will be presented.

This work is supported by NIST/Gaithersburg under contract number 50-DKNB-0-90072, and the US Army National Ground Intelligence Center, DAHC-90-96-C-0010.

### Introduction

The approach taken in the present work, to generate tunable THz, has been in use for a number of years.<sup>5</sup> In this method, a fixed frequency laser and a tunable millimeter-wave (MMW) source are both coupled into a high-frequency Schottky diode and the resulting sidebands are re-radiated out of said Schottky diode. Thus the resulting sideband radiation can be tuned by simply tuning the MMW source.

As there will typically be quite a large amount of non-sideband radiation, at the laser frequency, also present in the re-radiated beam, a method is often employed to "filter" the output – yielding only sideband radiation (often both upper and lower sidebands, though one will typically be noticeably weaker than the other).

Very recently, significant advances over the previous state-of-the-art output power achievable<sup>8</sup> from an SBG have been made.<sup>4</sup> These advances include use of newly available THz waveguides/embedding structures to improve the SBG-mixer-mode (we refer to as FM mode) conversion loss from 31 dB to 25 dB at 1.6 THz, and more significantly a new mode of operation for the SBG<sup>4</sup> where a conversion loss of 14 dB has been demonstrated at 1.6 THz. In this mode of operation, SBG-phase-modulation-mode (PM), the MMW radiation is used to directly modulate the THz impedance of the SBG element/block thus modulating its reflectivity. This avoids the loss associated with coupling THz currents through the Schottky diode whose parasitic parameters

“short-out” a large amount of the available THz energy.

In the present work the above advances in SBG technology are coupled with the recent advances in compact reliable THz laser sources.<sup>1,2</sup>

The remainder of this paper will: describe each of the key elements/technologies of the system, present measured and calculated performance results for each element, and then present the design for the final system to be constructed for NIST.

### Compact Laser Source

The compact laser source will be a DEOS SIFIR-50 FPL FSW. A photograph of this laser system (including its power supply and controller) is presented in Figure 1. The output power vs wavelength for this laser system (using a fixed hole output coupler) is presented in Figure 2, and the

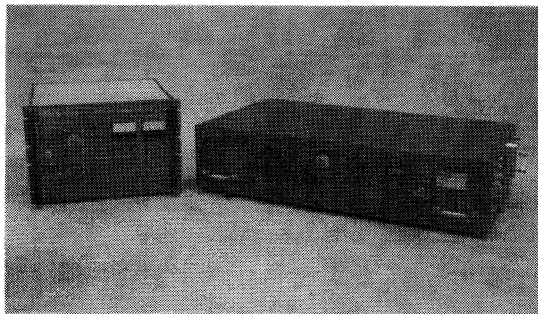


Figure 1: The SIFIR compact laser source.

spatial output mode obtained at 2.5 THz is shown in Figure 3. The short wavelength drop off in output power is due to the quartz output window used, which cuts-off at ~ 65  $\mu\text{m}$ . The slow drop-off at longer wavelengths is due to the FIR waveguide cut-off, and the low power spike at 236  $\mu\text{m}$  is due to the weak pump line for this laser line (9R6). The low frequency performance can be easily improved by using a larger waveguide diameter in the laser.

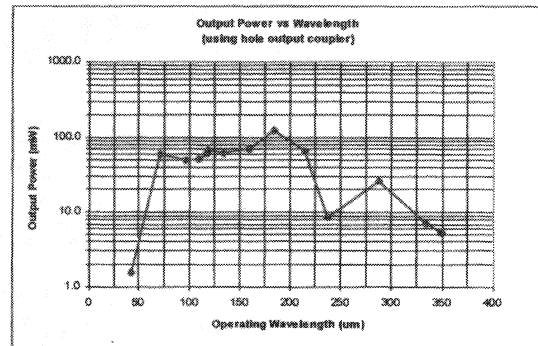


Figure 2: Output power vs wavelength for the laser source. (These data were obtained with a fixed hole output coupler. 2 - 3 times as much output power can in general be obtained at any given line by using a uniform output coupler.)

This laser system utilizes DEOS's permanently sealed-off pump laser technology, DEOS's compact high-vacuum-integrity high-stability THz laser technology, and an integrated design approach. The combination of these provides a reliable, easy to use THz laser.

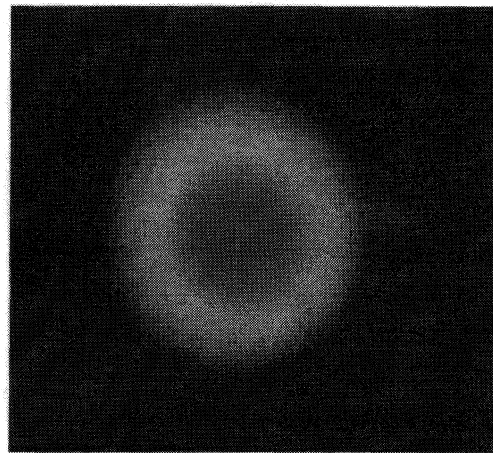


Figure 3: SIFIR spatial output mode at 118.83  $\mu\text{m}$ .

### Sideband Generator

The sideband generator used in this work is a University of Virginia 0.8  $\mu\text{m}$  Schottky varactor diode mounted in a machined/electro-formed block. The THz radiation is coupled into and out of the waveguide within the block via a diagonal

feedhorn and the MMW energy is coupled into the block via a standard connector. A photograph of the initial version of this SBG block is presented in Figure 4. The backshort is mechanically-tuned for optimal video response when changing laser lines.

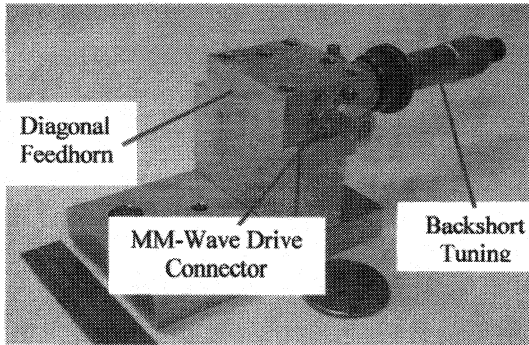


Figure 4: Photograph of the SBG mixer block.

Drawings of the inside of the block and of the planar whisker are presented in

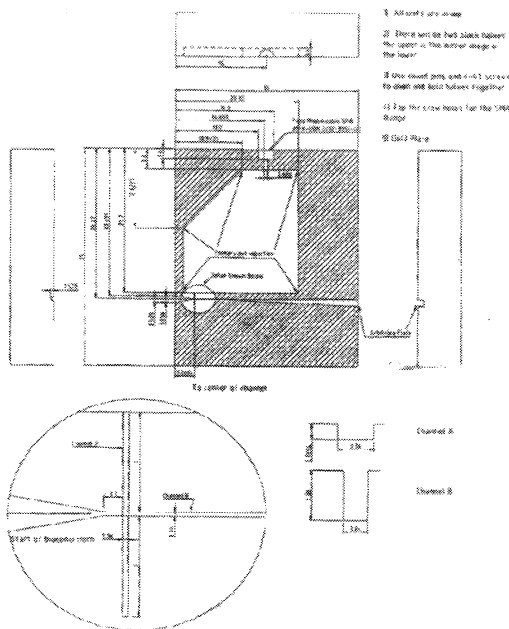


Figure 5: Drawing of the SBG mixer block.

Figure 5, and Figure 6, respectively. The planar whisker type used here is modeled after a technique developed for a 250 GHz tripler.<sup>6</sup>

As will be discussed later, this block was originally designed for operation at low (<18 GHz) offsets. During the present work minor changes were made to extend the block's operating range up to ~50 GHz, and simulations of the next generation design indicate operation up to 110 GHz. This represents a potential tuning range of 220 GHz around each laser line for 1<sup>st</sup>-order SBG operation.

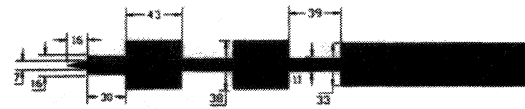


Figure 6: Drawing of the SBG contact/THz-coupling planar whisker. All dimensions are in  $\mu\text{m}$ .

### MMW Coupling to the SBG

To efficiently generate sideband power, it is necessary that both the THz and the millimeter-wave (MMW) energy be coupled to the SBG diode. To test and optimize this behavior a series of experiments and simulations were conducted. The initial tests were performed on an existing, far-from-optimal, SBG block, and the later measurements were made on the same block after minimal modifications were executed to improve its MMW performance. Following these measurements a series of simulations, and commensurate design changes, were performed so that future SBG blocks could be expected to operate at sideband offsets up to 110 GHz, with the MMW energy coupled into the SBG block via an Agilent 1-mm connector.

### - Initial MMW Testing

The SBG block used for this research was a prototype and was not designed for use at high microwave frequencies. A microstrip line on a Duroid substrate 40 mils thick was used to couple the MMW power to the diode, and a standard SMA connector (operating frequency range from DC to 18 GHz) was

used to connect to the block. In spite of this, initial tests were performed on the microwave coupling to the block, as shown in Figure 7. The curves in Figure 7 show the SBG block microwave reflection coefficient as the bias (and thus the diode impedance) is changed.

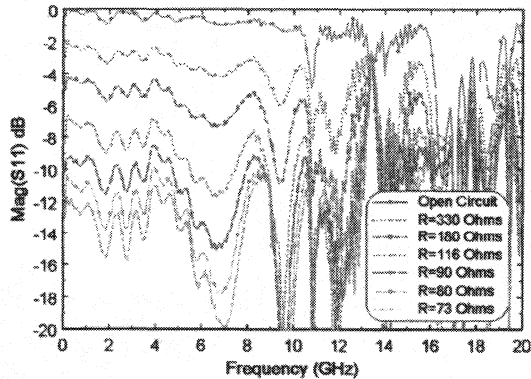


Figure 7: SBG block  $S_{11}$  measurements at a variety of diode bias points (bias currents).

When the diode is zero-biased the diode acts as an open circuit, and the amount  $S_{11}$  drops below 0 dB represents the microstrip line loss in the block. The line losses are small up to about 10 GHz, at which point resonances in the reflection coefficient begin to appear. Above about 15 GHz the microwave coupling degrades rapidly. The microwave coupling problems for this block are caused by resonances in the electrically-large microwave cavity and by discontinuities and air-gaps in the microstrip line. In order to solve these problems, the MMW circuit needed to be redesigned.

#### - SBG MMW Circuit Modification

In order to extend the MMW bandwidth for this project it was decided to modify the block again to address some of the MMW coupling issues. To do this, the SMA connector was replaced by a V-connector (operating frequency range from DC to 60 GHz). Also, the 40 mil Duroid substrate (dielectric constant 10.2) was replaced by a much shorter 3 mil thick quartz substrate (dielectric constant 3.8). The

modification is pictured in Figure 8. While this modification was expected to solve some of the problems seen previously, the MMW cavity was still much larger

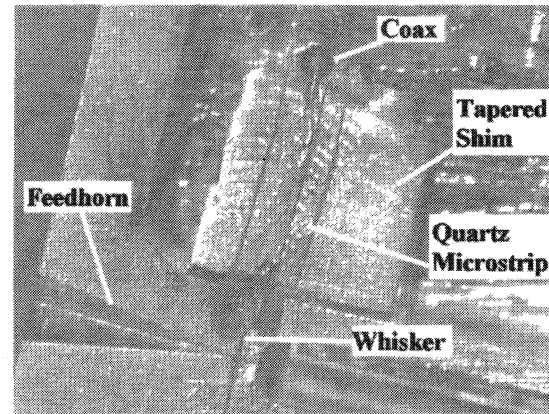


Figure 8: Internal view of the modified SBG block.

than desired for high frequency operation, a point that will be discussed more fully in the MMW simulations section.

#### - Improved-Block MMW Testing

MMW testing was performed on the modified SBG block, the results of which are shown in Figure 9. The upper curve (for a zero-biased diode) shows that the SBG

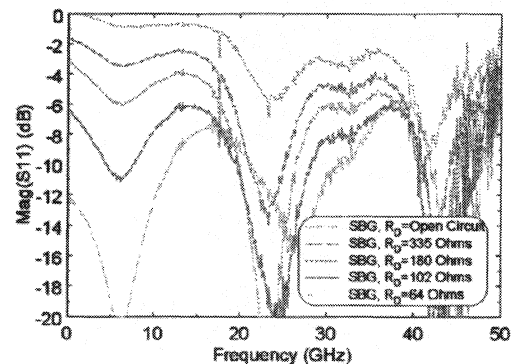


Figure 9:  $S_{11}$  measurements of the improved SBG block.

block loss is relatively flat up to 50 GHz (the upper limit of the network analyzer configuration used), although there are soft

resonances at 25 and 40 GHz. A comparison of this performance with the performance before the MMW circuit modification (Figure 7) reveals the dramatic decrease of line loss at high frequencies.

In order efficiently generate sidebands from the laser the MMW signal applied to the SBG must be able to modulate the diode bias, thus allowing phase modulation of the THz to occur. Since the change in capacitance of the diode with changing bias point causes the change in reflected phase, a figure-of-merit that allows us to gauge the ability of the MMW to modulate the diode is the MMW responsivity of the SBG. This is defined as the ratio of diode video response to the applied microwave power. The video response is determined by measuring the change of the diode bias voltage when microwave power is applied with the diode bias current fixed at a forward current of 0.6 mA. This bias point was found suitable for sideband generation during previous experiments.<sup>4</sup> Figure 10 shows the measured responsivity of the SBG block for

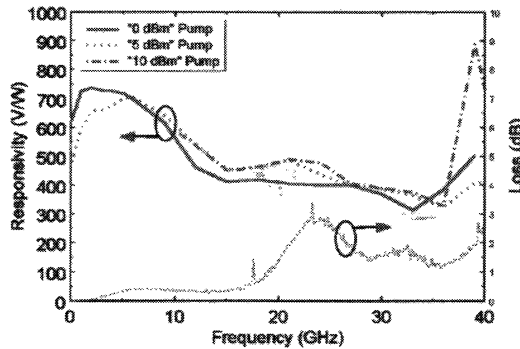


Figure 10: Measured MMW responsivity of the SBG.

several different MMW power levels. The MMW power was found to effectively modulate the diode bias all the way up to 50 GHz. The responsivity is (to within measurement error) constant as the MMW power changes, which is expected since the MMW pump power is still quite low. The

scatter in the data at high frequencies is due to a rapid decrease in available MMW power from the network analyzer at high frequencies and also to the video response measurement accuracy of  $\pm\frac{1}{2}$  mV. Above 40 GHz the measured video response was on the order of the measurement accuracy.

#### - 110 GHz MMW Simulations

In order to determine the proper configuration for future SBGs and also to examine the limitations of the MMW coupling bandwidth, MMW coupling simulations were performed using Ansoft's HFSS, a finite-element analysis package. The key to achieving MMW coupling to the SBG diode is to avoid line discontinuities and cavity resonances. Figure 11 shows transmission plots for several MMW circuit

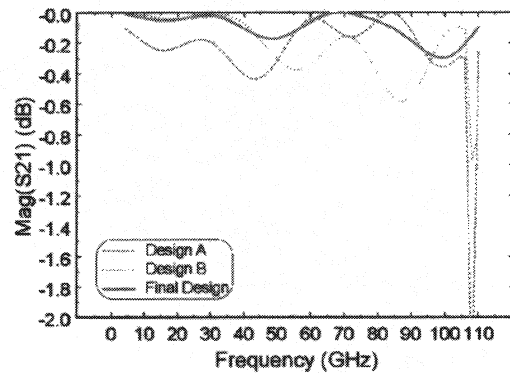


Figure 11:  $S_{21}$  simulation results for the future-design SBG block.

configurations that were simulated. The main difference between the various curves is the size of the cavity. By reducing the cavity size sufficiently the higher-order modes at 110 GHz can be cutoff, and the simulations indicate that the coupling of microwave power to the diode is possible up to 110 GHz. The final design uses 5 mil quartz and a cavity configuration that can be easily machined using standard milling techniques. By using this cavity design along with an Agilent 1-mm coaxial connector (operating frequency range from DC to 110 GHz) the

microwave operating range of the SBG can be extended all the way to 110 GHz.

### THz Coupling to the SBG

In order to understand the THz coupling to the SBG diode, a series of video

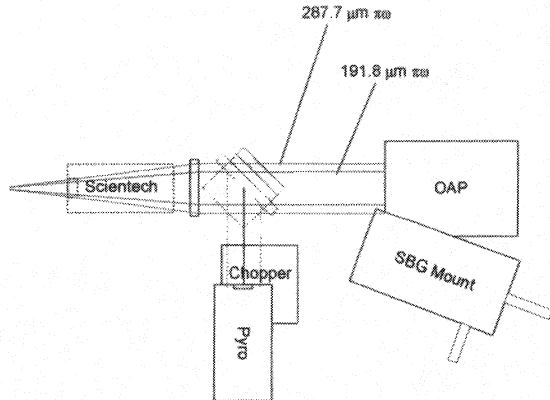


Figure 12: Diagram of the THz response experimental set-up.

responsivity measurements vs THz laser frequency were performed.

A diagram of the optical set-up is presented in Figure 12, and a photograph of the layout is shown in Figure 13. At each

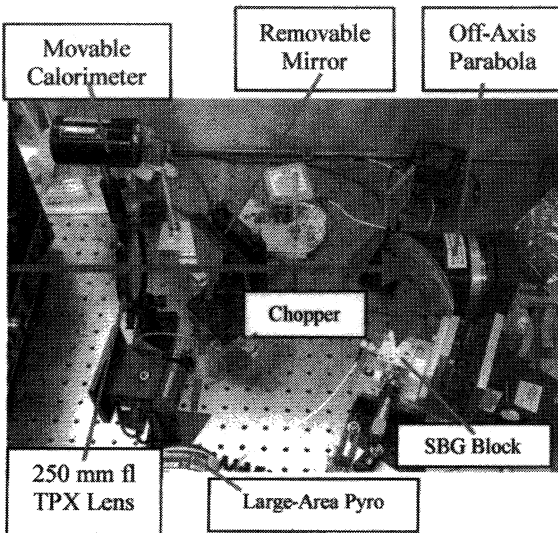


Figure 13: Photograph of the THz response experimental set-up.

test wavelength a measure of the output power from the laser was made and then an attenuator was added to keep the THz power

at the diode in the 3-10 mW range. The laser output powers were measured with a Sciencetech calorimeter and then calibration corrected.<sup>7</sup>

The results of the THz measurements are presented in Figure 14. The “Normalized Response” data were normalized at 1.6 THz, and the “Re-Normalized Response” data are the Normalized data with a  $1/v^2$  dependence factor applied to remove the natural response characteristic response of the diode (to illustrate the block’s THz performance).

The low frequency cut-off is expected due to the waveguide dimensions but the slowness of the high-frequency

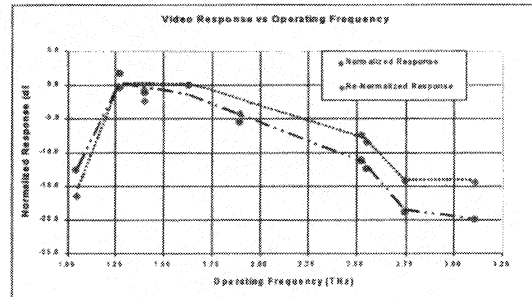


Figure 14: THz response measurement results. The lines are only intended to be an aid to the reader and do not represent a “best-fit” of any kind.

response is surprising. The gradual high-frequency roll-off, combined with improved SBG conversion efficiency, suggests that a large portion of the THz region could be covered, with multi- $\mu$ W output, with only 1 or 2 SBG blocks. This makes the waveguide block approach much more attractive than previously thought.

In the past SBG’s were typically corner-cube mounted. This provided wide THz bandwidth through tuning of the corner-cube and antenna but did not provide the flexibility in embedding impedance offered by the waveguide mounting. The above THz measurements, coupled with simulation results to be presented later, indicate that the

waveguide approach is indeed feasible and in fact may be preferable.

### Quasi-Optical Diplexer

To separate the drive laser from the sideband output some type of diplexing device will be required. A number of alternatives for this function were considered including: a series of etalon diplexers,<sup>8</sup> a tunable etalon diplexer, a Mach-Zender diplexer,<sup>9</sup> and a Martin-Puplett<sup>10</sup> diplexer.

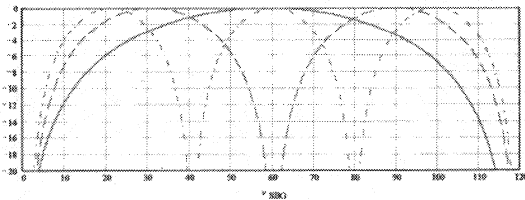


Figure 15: Diplexer SBG frequency coupling efficiency plot. The vertical axis is the SBG-to-output port transmission in dB, and the horizontal axis is the SBG offset frequency in GHz.

The Martin-Puplett topology was selected for a number of reasons including: capability of accommodating either laser polarization through simple adjustment of the first grid and the diplexer spacing, performance of available grids throughout the THz, availability of components, and cost.

The theoretical performance vs sideband offset frequency is presented in Figure 15. The three plots shown there are for different settings of the diplexer spacing, and illustrate the capability of very wide band performance and end-of-band operation via user tuning of the diplexer spacing.

### System Design & Performance Projections

The system design will combine the laser, diplexer, and SBG to form a reliable, easy to use, tunable THz source.

A drawing of the system is shown in Figure 16, and

Figure 17. The SBG and diplexer are integrated directly on the top of the laser housing. The laser housing is ~ 100 cm x 50 cm x 25 cm. The diplexer and 5-axis mount for the SBG are sufficiently small that the remainder of the laser top can be used for additional experimental space.

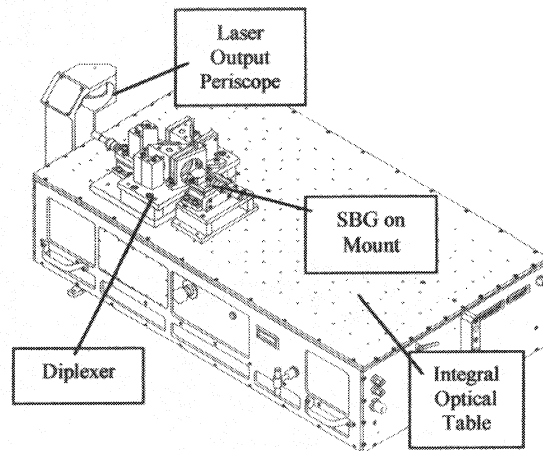


Figure 16: Design drawing of the system.

It is desirable that the optical system for coupling the laser to the SBG be constant vs operating wavelength. We have devised such an optical system. The beam propagation for the optical system is

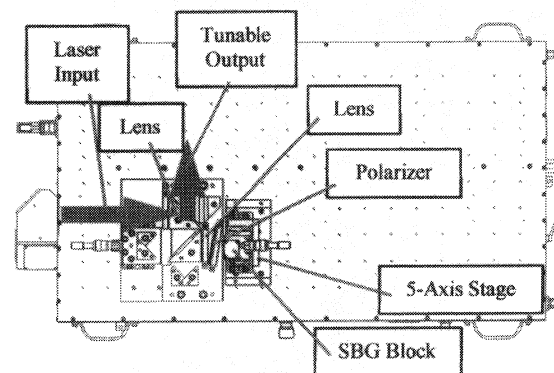


Figure 17: Plan view of the system.

presented in Figure 18. While in that plot it appears that the beam size at the SBG is independent of wavelength, in fact there is some wavelength dependence. The wavelength dependence of the waist at the SBG input is presented in Figure 19. This

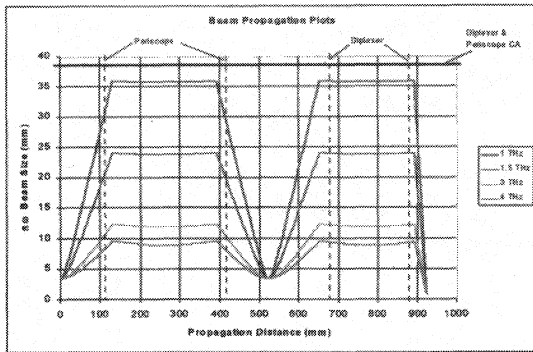


Figure 18: Beam propagation plots.

dependence is due to some slight non-symmetry in the design and corrections due to operating with low  $f\#$ .<sup>11</sup>

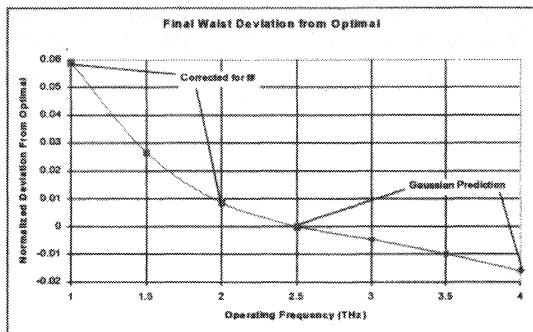


Figure 19: SBG-Coupling beam size predictions vs operating frequency. Note: the low frequency calculations include a correction for small  $f\#$ <sup>11</sup> and the higher frequency predictions are paraxial Gaussian propagation results.

### - Sideband Conversion Efficiency Modeling

It is desirable to make some estimates of output power vs frequency achievable with the envisioned system. To that end, a model of the SBG efficiency vs operating frequency was developed.

This model is broken into two distinct operating regimes: PM-mode operation, and FM-mode operation. It is expected that the achievable PM-mode range will be somewhat limited and that where this

mode of operation rolls-off, the more conventional, FM-mode will dominate.

To estimate the PM-mode performance vs frequency the SBG was modeled using the post-in-a-waveguide analysis of Eisenhart. Error! Bookmark not defined.

The equivalent circuit for the SBG is shown in Figure 20. Note that this equivalent circuit does not model the effect of finite bandwidth of the low-pass filter fabricated on the planar whisker, and assumes the guide is shorted at the edge of the waveguide.

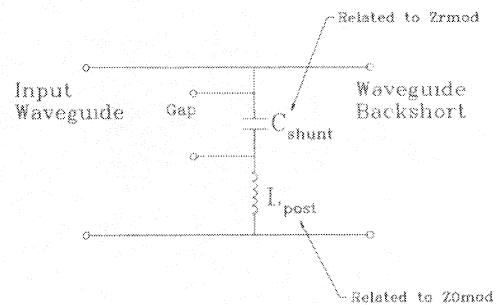


Figure 20: Circuit model of the SBG/block.

Using this simplified model of the SBG and the predicted capacitance variation for the varactor used (i.e. from 0.4 fF to 2.5 fF) the amount of phase modulation achievable at a given THz frequency (where the backshort position is optimized for each THz frequency) is calculated. (For 1<sup>st</sup>-order SBG operation no more than 180 degrees of PM is desired). These results were then normalized to the 14 dB measured result at 1.6 THz to yield the dashed maroon curve found in Figure 22.

Since the output power of the laser is known, the SBG THz coupling efficiency for the block was measured, and the PM conversion efficiency has been estimated, it is now possible to estimate the output power one would expect when operating the designed system in PM mode. However it is expected that the conversion efficiency will saturate with increasing laser power. At this time there is no existing data on this effect, and so as an approximation, it was assumed that the efficiency would be constant up to

20 mW of input power and roll-off by 6 dB by the time the laser power

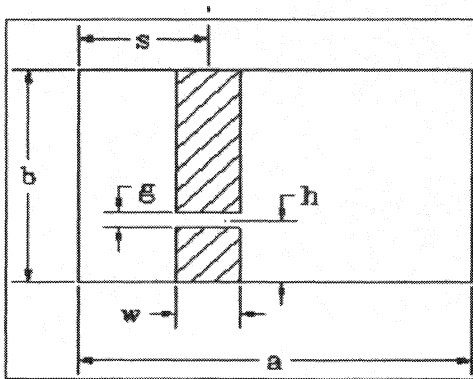


Figure 21: Waveguide/post physical model. *a* and *b* are the dimensions of the waveguide (160 x 40  $\mu\text{m}$ ); *s* is the distance from the waveguide wall to the diode post (80  $\mu\text{m}$ ); *g* is the gap between the waveguide post and the end of the wide section of the whisker (10  $\mu\text{m}$ ); and *h* is the height of the diode mounting post –  $\frac{1}{2} g$  (0.4  $\mu\text{m}$ ), and *w* is the width of the post and whisker end section just prior to the narrowed contact area (taken to be 40  $\mu\text{m}$  in this model for improved performance at higher frequencies).

is increased to 100 mW. When all of these factors are used the resulting prediction is that shown in the solid blue curve of Figure 22.

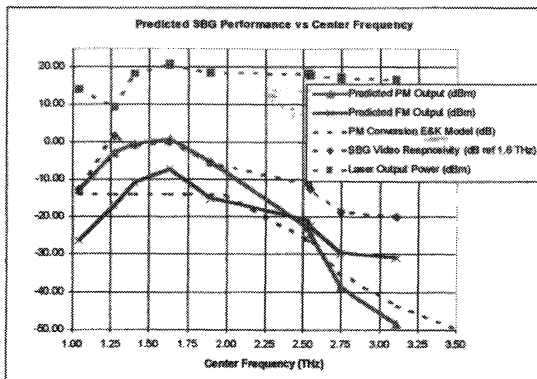


Figure 22: Measured & Predicted Laser/SBG system performance vs center frequency. The laser output power vs operating frequency and normalized SBG responsivity are included for illustration.

It is expected that at the point where the PM-mode of operation falls below the estimated FM-mode of operation, the FM-mode output power will dominate. To estimate this, the THz responsivity and a conservative 28 dB conversion loss at 1.6 THz (measured result in the waveguide SBG was approximately 25 dB but this result was for a mixer diode) were multiplied to yield the solid red curve of Figure 22.

These data are quite encouraging. They suggest that even without using multiple SBG blocks, each optimized for a given band, it should be possible to obtain multi- $\mu\text{W}$  tunable THz output over a very broad range and mW tunable output over a more restricted range.

### Conclusions

In this work recent developments in SBG and laser technology have been brought together to yield a design with potentially impressive output power over the entire THz regime.

The experimental data, simulations, and resulting design, should yield an easily used, tunable THz source with  $>10$ 's of  $\mu\text{W}$  of output power over a very broad range, and even possibly mW output power over a more narrow range. The mW levels should also be realizable throughout much of the THz by using optimized SBG blocks at the desired THz center frequencies.

While the present design was evaluated for 1<sup>st</sup>-order SBG only, 2<sup>nd</sup>-order operation could also be used to extend its MMW tuning range at any given laser line.

This system should prove to be an excellent source for spectroscopy and LO applications.

### Acknowledgements

The authors would like to acknowledge the contributions of D. Porterfield to this project.

## References & End Notes

- <sup>1</sup> E. R. Mueller, W. E. Robotham, Jr., R. P. Meisner, R. A. Hart, J. Kennedy, and L. A. Newman, "2.5 THz Laser Local Oscillator for the EOS Chem 1 Satellite," Proc. 9<sup>th</sup> Int. Symp. Space Terahertz Technol., p. 563 (1998)
- <sup>2</sup> E. R. Mueller, J. Fontanella, & R. W. Henschke, "Stabilized, Integrated, Far-Infrared Laser System for NASA/Goddard Space Flight Center," Proc. 10<sup>th</sup> Int. Symp. Space Terahertz Technol., (2000)
- <sup>3</sup> D. S. Kurtz, J. L. Hesler, T. W. Crowe, and R. M. Weikle, II, "Millimeter-Wave Sideband Generation Using Varactor Phase Modulators," IEEE Microwave & Guided Wave Lett., **10**(6), 245 (2000)
- <sup>4</sup> David S. Kurtz, Sideband Generation for Submillimeter Wave Applications, Doctoral Dissertation, University of Virginia, Charlottesville, May 2000
- <sup>5</sup> H. R. Fetterman, P. E. Tannenwald, B. J. Clifton, W. D. Fitzgerald, and N. R. Erickson, "Far-ir heterodyne radiometric measurements with quasioptical Schottky diode mixers," Appl. Phys. Lett., **33**, 151 (1978); D. D. Bicanic, B. F. J. Zuidberg, and A. Dymanus, "Generation of continuously tunable laser sidebands in the submillimeter region," Appl. Phys. Lett., **32**(6), 367 (1978)
- <sup>6</sup> J. Thornton, C.M. Mann, and P. de Maagt, "Optimization of a 250-GHz tripler using novel fabrication and design techniques," IEEE MTT, **46**(8) 1055 (1998)
- <sup>7</sup> F. B. Foote, D. T. Hodges, and H. B. Dyson, "Calibration of Power and Energy Meters for the Far Infrared/Near Millimeter Wave Spectral Region," Int. J. IR & MMW, **2**(4), 773 (1981)
- <sup>8</sup> E. R. Mueller, and J. Waldman, "Power and Spatial Mode Measurements of Sideband Generated, Spatially Filtered, Submillimeter Radiation," IEEE MTT, **42**(10) 1891 (1994)
- <sup>9</sup> N. R. Erickson, "A Directional Filter Diplexer Using Optical Techniques for Millimeter to Submillimeter Wavelengths," IEEE MTT, **25**, 865 (1977)
- <sup>10</sup> D. H. Martin, and E. Puplett, "Polarised Interferometric Spectrometry for the Millimetre and Submillimetre Spectrum," Infrared Phys., **10**, 105 (1969)
- <sup>11</sup> G. P. Agrawal, and D. N. Pattanyak, "Gaussian beam propagation beyond the paraxial approximation," J. Opt. Soc. Am., **69**(4), 575 (1979)